Drawdown Behavior of a Horizontal Well with Transverse Fractures in a Shale Gas Reservoir

Figure 4 shows a plane view of an SRV defined by a horizontal well with 8 transverse fractures. The SRV extent is drawn with approximately one half of the fracture spacing beyond the fractures at the heal and toe of the well and approximately one quarter of the fracture spacing beyond the fracture tip.

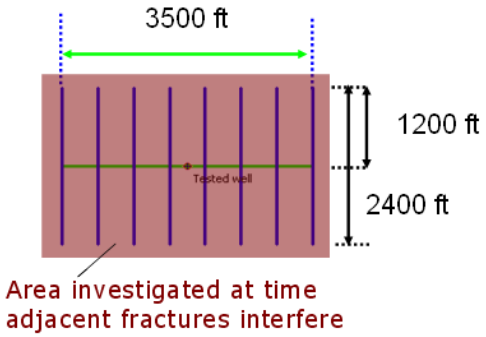

Figure 4. Plane View of SRV

A sensitivity study showing the effect of permeability on the drawdown behavior for an SRV located in an effective infinite reservoir is shown in Fig. 5. The graph on log-log axes shows a pair of curves representing the pressure change and its derivative with respect to the logarithm of time (logarithmic derivative) color coded for each of the permeability values ranging from 1 md to 100 nanodarcy (0.0001 md). The study is shown as drawdown so that key features in the response are clearly visible. Table 1 lists the parameters used in the simulation.

In early time fracture storage is seen in both pressure change and derivative aligned in a unit slope trend. This is followed by a hump representing the transition to pseudolinear flow marked by a half slope trend in both curves. During pseudolinear flow each fracture produces independently with the reservoir fluid flowing mainly perpendicular to the fracture planes with a small fraction of the flow coming to the fracture tips.

During pseudolinear flow, the shale permeability is related to the fracture half-length by:

$$n_f x_f \sqrt{k} = \left(\frac{4.064 q_o B_o}{m_{lf} h}\right)\left(\frac{\mu_o}{\phi c_t}\right)^{1/2} \quad \text{for oil}$$

$$n_f x_f \sqrt{k} = \left(\frac{724 q_g B_g}{m_{lf} h}\right)\left(\frac{\mu_g}{\phi c_t}\right)^{1/2} \quad \text{for high pressure gas with rate in Mscf/d} \qquad \text{..... (3)}$$

$$n_f x_f \sqrt{k} = \left(\frac{40.93 qT}{m_{lf} h}\right)\left(\frac{1}{\phi \mu c_t}\right)^{1/2} \quad \text{for gas using } m(p) \text{ with rate in Mscf/d}$$

Where n_f is the number of transverse fractures, all assumed to have the same half-length, x_f.

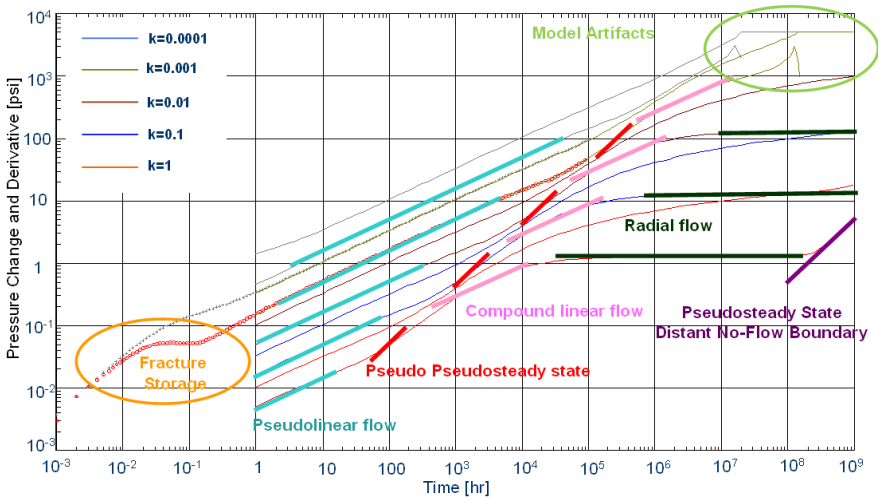

Figure 5: Sensitivity to permeability for well and reservoir properties in Table 1.

The duration of the pesudolinear flow regime is governed by the diffusivity coefficient for the shale gas reservoir. Fig. 5 shows that this flow regime can last for several logarithmic time cycles. During pseudolinear flow, the pressure disturbance penetrates the formation in the direction perpendicular to the fracture planes. Pesudolinear flow ends at t_{eplf} when the pressure disturbances from two adjacent fractures interfere, and this is seen as an upward departure from the pseudolinear flow trend. In the absence of significant adsorption, the time this will occur is given by

$$t_{eplf} = \frac{948 \pi \phi \mu c_t (x_s/2)^2}{4k} \qquad (4)$$

where x_s is the fracture spacing in ft [Ehlig-Economides (1992)]. For gas wells t_{eplf} must be determined using the average pressure in the fracture drainage area to compute viscosity and compressibility.

Al-Kobashi et al (2006) showed that pseudoradial flow can occur after pseudolinear flow if the fracture spacing is large compared to the fracture half-length. However, in shale gas wells this is seldom the case. Instead, each fracture continues to produce from its own effective drainage area bounded by the virtual no flow boundary between adjacent fractures. If multiple MTFWs are drilled with spacing sufficiently close that their SRVs touch, then virtual closed boundaries will exist opposite each fracture tip. In that case each fracture will go into pseudosteady state flow, and the pressure in the SRV will drop linearly with time. Instead, if no nearby wells provide virtual boundaries opposite the fracture tips, then each fracture produces in a pseudo pseudosteady state like what is labeled as such in Fig. 5.

We use the term pseudo pseudosteady state because the small part of the fracture drainage area boundary opposite the fracture tips is not actually closed. As a result, the pressure change is not quite linear with time, and the derivative trend may be slightly less than unit slope. Whether pseudosteady or pseudo pseudosteady state flow occurs, in either case the SRV pore volume, $\phi V_{sr}=V_p$ is related to the pressure change versus time as [Lee, Rollins, and Spivey (2003)]

$$\frac{dp_{wf}}{dt}=\frac{0.234qB}{V_p c_t} \text{ for oil}$$
$$\frac{dp_{wf}}{dt}=\frac{41.7qB}{V_p c_t} \text{ for high pressure gas (rate in MSCF/d)} \quad \text{..... (5)}$$
$$\frac{dm(p_{wf})}{dt}=\frac{2.36qT}{\bar{\mu}\bar{Z}V_p c_t} \text{ for any pressure gas (rate in MSCF/d)}$$

The derivative dp_{wf}/dt is easily determined from the log-log graph as the product of the logarithmic derivative and time. A careful look at Figure 5 reveals that the trends marked pseudo pseudosteady state all follow the same approximately unit slope line because each represents the same value for V_{sr}. Figure 6 shows a diagram of the flow to each fracture during pseudo pseudosteady state flow.

Table 1. Sensitivity Study Model Inputs

Reservoir properties		
h, ft	Pay zone thickness	30
ϕ	Porosity	0.1
T, ºF	Reservoir temperature	212
p_i, psia	Initial reservoir pressure	5000
Well and stimulated fracture properties		
L_w, ft	Well length	3200
n_f	Number of fractures	8
x_f, ft	Half-length of fractures	1200
r_w, ft	Wellbore radius	0.3
z_w, ft	well vertical distance to reservoir bottom	15
PVT properties		
γ_g	Gas specific gravity	0.7
Well and wellbore parameters		
Wellbore model	No wellbore storage	
s	Skin factor	0
Fracture model	infinite-conductivity	
Desorption parameters		
p_L, psia	Langmuir pressure	2000
ρ_{ads}, g/cc	Adsorption density	0.1

When the average pressure in the SRV approaches that at the wellbore, the fluid in the SRV is effectively depleted. At this time the SRV becomes a sink producing from the remainder of the drainage volume of the MTFW. If the MTFW drainage area is much larger than the SRV, compound linear flow will occur first followed by pseudoradial flow to the SRV. Although compound linear flow, like pseudolinear flow, exhibits a ½ slope trend, its duration is less than one log cycle. When ½ slope behavior is observed for more than one log cycle in time, it represents pseuudolinear flow. Once the outer boundary of the MTFW is sensed, the well will reach final steady or, more likely, pseudosteady state flow.

The flow regimes described in the previous paragraph, while mathematically interesting, in almost all shale gas reservoirs they are not likely to happen in any economically meaningful production time, even after many years. Flow in the SRV effectively represents a significant skin on the flow from outside the SRV to the created fractures. Therefore, the flow rate is likely to drop below the economic rate before the end of pseudo pseudosteady state flow, or, if the fracture spacing is too large, before the end of pesudolinear flow. For this reason wells should be spaced sufficiently close that the SRVs are effectively adjacent, and our well design approach puts the focus only on depleting the SRV as though it is equivalent to the drainage volume for the MTFW.

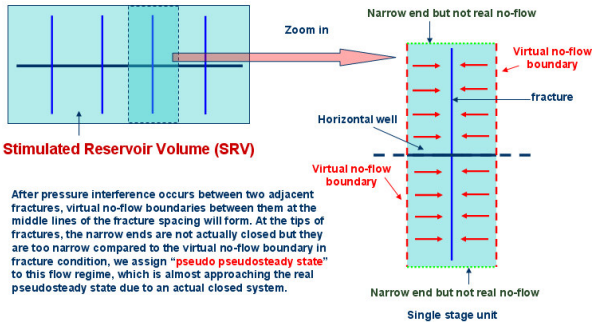

Figure 6: Pseudo pseudosteady state

During pseudolinear and pseudo pseudosteady state flow each fracture independently drains its own drainage area, and the total flow from the well is the sum of the flow to each of the fractures. Therefore, the well design treats the MTFW as the sum of n_f fractures, each draining an area $A_f = 2(x_f + 1/4x_s)x_s$. with width x_s and length $2(x_f + 1/4x_s)$. The pore volume of the SRV is given by

$$\phi V_{sr}=\phi n_f A_f h=\phi n_f\left[2\left(x_f+\frac{x_s}{4}\right)x_s\right]h \quad (6)$$

Figure 7 shows a sensitivity study varying the fracture spacing for a given permeability. As the fracture spacing narrows, pseudo pseudosteady state behavior starts sooner and lasts longer. In some field data the fracture spacing is small enough that the entire production history is dominated by this flow regime. This may represent spacing between fracture stages, between

multiple fractures per stage, or even an effective fracture spacing of what is loosely called complexity. The model inputs for this study are shown in Table 2 and represent properties similar to reported values for the Haynesville Shale.

Table 2. Sensitivity Study Model Inputs for Figures 7 and 11

Reservoir properties		
h, ft	Pay zone thickness	50
ϕ	Porosity	0.05
T, ºF	Reservoir temperature	350
p_i, psia	Initial reservoir pressure	9000
Well and stimulated fracture properties		
L_w, ft	Well length	2000
n_f	Number of fractures	6-81
x_f, ft	Half-length of fractures	500
r_w, ft	Wellbore radius	0.3
z_w, ft	well vertical distance to reservoir bottom	25
PVT properties		
γ_g	Gas specific gravity	0.7
Well and wellbore parameters		
Wellbore model	No wellbore storage	
s	Skin factor	0
Fracture model	infinite-conductivity	
Desorption parameters (not considered)		

Figure 8 summarizes the flow regimes seen in the sensitivity studies. Figure 9 shows the typical long term pressure drawdown behavior of MTFWs corresponding to Figure 8.

In reality, if wells are spaced such that one SRV is adjacent to the next, then pseudo pseudosteady state and pseudosteady state become the same. In this case the well rate can be estimated as the rate forecast for each fracture multiplied by the number of fractures. As such our simplified model for each fracture considers only two flow regimes: pseudolinear flow until the time of inter-fracture interference, and pseudosteady state after that.

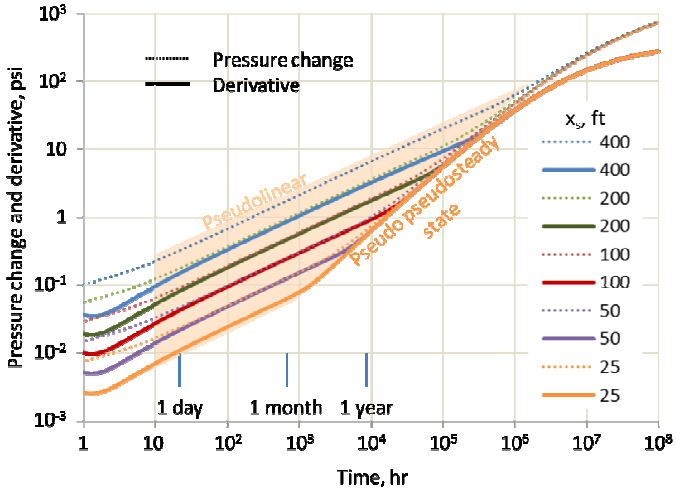

Figure 7: Sensitivity study for k = 0.0001 md showing the effect of fracture spacing on the start and duration of pseudo pseudosteady state flow

Figure 10 shows the impact of adsorption on the pressure drawdown response. Effectively, gas adsorption delays the pressure penetration as an effective time shift. To take this into account, we define the *adsorption index* (I_{ads}) to quantify this effect. The definition of I_{ads} is the ratio of pressure investigation time with adsorption to its corresponding investigation time without adsorption.

$$I_{ads} = t_{ads}/t_{noads} \tag{7}$$

A large number of simulations were run to establish the following correlation for the adsorption index as a function of adsorption parameters and reservoir properties.

$$I_{ads} = C_{ads}\rho_{ads} + 1 \tag{8}$$

where the adsorption coefficient, C_{ads}, is given by:

$$C_{ads} = C(\phi, p_i, p_L) = A_c \frac{1}{\sigma\sqrt{2\pi}} \exp\left(-\frac{\log^2(p_L/p_i)}{2\sigma^2}\right) \tag{9}$$

for $\sigma = 0.6644$ and $A_c = (6875.34/p_i + 2.4298\times10^{-4}p_i - 0.1992)\phi^{1.0215}$. The correlation applies for $0.01 < \phi < 0.1$, 0.01 g/cc $< \rho_{ads} <$ 0.1g/cc, 1000 psi $< p_i <$10000 psi and $p_i/10 < p_L < 10p_i$. When parameters are outside the above ranges, simulation is recommended to determine the adsorption index.

The previous observations enable calculation of the approximate rate decline behavior for a MTFW shale gas well with equally spaced fractures of a given fracture half-length and given reservoir and adsorption properties. During pseudolinear flow the gas flow rate to a single transverse fracture under constant pressure production is given by

$$q_g = \frac{kh[m(p_i)-m(p_{wf})]}{1424(\pi/2)T}\left[\frac{0.000264\pi k(tI_{ads})}{\phi(\mu c_t)_i x_f^2}\right]^{(-1/2)} \tag{10}$$

and during pseudo pseudosteady state flow, the gas flow rate for constant pressure production is approximated by

$$q_g = q_{gi}e^{-D_i t} \tag{11}$$

where D_i is given by $D_i = q(t_{eplf})/\left(\phi V_{sr}/B_{gi} - Q(t_{eplf})\right)$. These equations are used for the well design approach in the next section.

Rate Decline Behavior of a Horizontal Well with Transverse Fractures in a Shale Gas Reservoir

Very likely during much of the time the well is on production it will be produced with a variable, not a constant, rate. In that case the rate-normalized pressure (RNP) computed as $[p_i - p_{wf}(t)] / q(t)$ and its derivative with respect to the logarithm of the material balance time, $t_e = Q(t)/q(t)$ provides a virtual drawdown response for production at a constant reference rate. When graphed with logarithmic axes as a function of material balance time, the RNP and its derivative following the same behavior as the constant rate drawdown response, and the flow regimes discussed previously are clearly visible. Alternatively, the pressure normalized rate, or transient productivity index, computed as the reciprocal of the RNP, which is also called the reciprocal productivity index, provides a virtual rate decline for production at a constant flowing pressure. When graphed with logarithmic axes as a function of material balance time, the pressure normalized rate shows a straight trend with negative unit (-1) slope under pseudo pseudosteady and pseudosteady state flow conditions, and this behavior is analogous to exponential rate decline.

Figure 11 shows rate decline and cumulative production for the same cases as are shown in Fig. 7 for flow at a constant pressure of 100 psi. At the 400 ft spacing, the well produces in pseudolinear flow for more than 12 years (105,000 hr) from 6 fractures. In contrast, the well with effectively 25 ft fracture spacing (81 fractures) produces the same cumulative production in about one month (720 hr). All of the well models produce about 53% of the gas in place before inter-fracture interference occurs. Additionally, the arrow shows that for an economic limit rate of 100 MSCF/d, all of the well models achieve a recovery factor greater than 95% of the SRV pore volume. Comparing Figs. 7 and 11 shows that the time of inter-fracture interference (end of pseudolinear flow) is the same, independent of the flow rate history, as expected because Eq. 4 is not dependent on the flow rate.

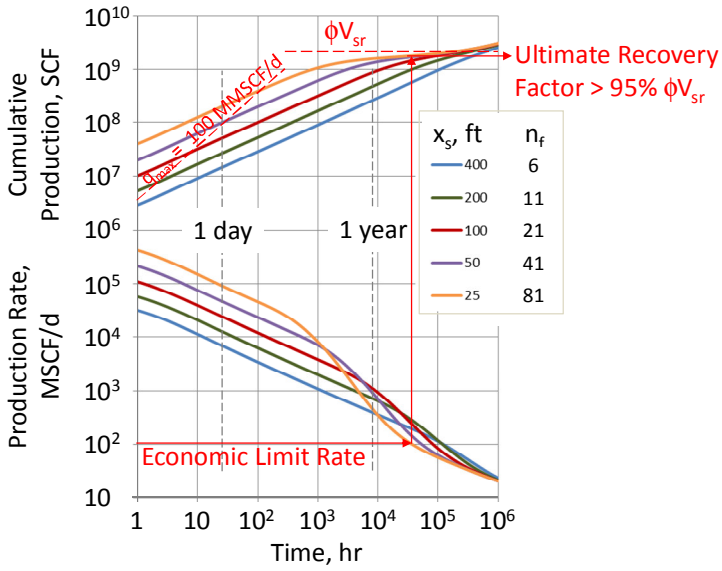

Figure 11: Rate decline and cumulative production for model inputs in Table 2.

When flow is started with a step drop in the wellbore pressure from initial reservoir pressure to a constant flowing wellbore pressure, the model gives nearly infinite rates for very early time. The dashed lines in the top left of the graph in Fig. 11 approximate constant rate production that would occur very early in time as the well naturally chokes back the flow. The assumed limit rate is consistent with 4.5 in production tubing. Once the modeled well cumulative production exceeds the constant rate cumulative production, the well will remain at the target flowing pressure, and will assume the modeled rate decline behavior.

The number of fractures may be interpreted as one fracture per fracture stage, multiple parallel fractures per stage each initiated from a perforation cluster, or as fracture "complexity". However, each fracture or effective fracture has the given fracture half-length, for these cases 500 ft.

Approach for Designing an MTFW

The approach we have developed for design of an MTFW assumes that there is a reliable estimate for the shale permeability and that analysis has been done to quantify adsorption parameters. Also needed are the shale thickness and porosity and

reservoir pressure and temperature, as well as economic parameters including cost estimates for drilling the vertical well segment, the cost per foot for horizontal drilling, the cost of each fracture (for an assumed fracture half-length), the discount rate and any royalty payments to be charged against production revenue at an assumed natural gas selling price. The goal is to arrive at a profitable design that pays out by a target payout time, and that will achieve at least a 50% recovery factor over the life of the well.

One approach for the well design could be to assume a target SRV shape. As in Eq. 6, the SRV length is approximately the horizontal well length, the SRV height is the shale thickness, and the SRV width corresponds to approximately twice the fracture half-length. With this approach there is a need to decide on the number of fracture stages. The minimum number of fracture stages should be sufficient to payout the well within a specified period and provide sufficient return on investment over its time on production. However, an additional objective could target a recovery factor for the well. To recover a significant fraction of the gas in place in the SRV it is essential that inter-fracture interference occurs during its time on production.

After inter-fracture interference has occurred, the average pressure in the SRV drops linearly with material balance time. If production from adjacent fractures never intersects over the life of the well, the sections of the SRV between the fractures will remain at the original reservoir pressure as by-passed resource. After interference, the well productivity becomes constant, but if the well is producing at a constant wellbore pressure, the rate will decline exponentially.

As an approximation the design program assumes the well is to be produced at constant pressure and computes the rate decline for each fracture as pseudolinear (Eq 10) until the time of pressure interference between adjacent fractures and as exponential decline thereafter (Eq 11). The total well rate decline is that of an individual fracture multiplied by the number of fractures. With this approach, we are able to forecast the well rate, cumulative production and discount production revenue.

$$PV_{payout} = \sum_{i=1}^{payout} \frac{n_f P_g (1 - r_{royalty}) Q_{a_i}}{(1 + r_{dis})^i} \tag{12}$$

Where P_g is the gas price in \$/Mscf, $r_{royalty}$ is the fraction to be paid as royalty, Q_{ai} is cumulative production during every single year in Mscf, and r_{dis} is the discount ra te. Payout occurs when the discount production revenue is equal to the capital cost of the well.

$$PV_{payout} = dC_{uvw} + n_f \left(x_s C_{uhw} + C_{ufrac} \right) \tag{13}$$

where n_f is the minimum fracture number needed, d is the vertical depth of the well in ft, C_{uvw} is the unit vertical drilling cost in \$/ft, C_{ufrac} is the single fracture cost in \$, C_{uhw} is the unit horizontal drilling cost in \$/ft and x_s is the fracture spacing in ft. After that production can continue as long as production revenue exceeds the operational cost.

Once all essential parameters have been specified, the design process starts with a recommendation for the fracture spacing based on an input value for the interference time, t_{eplf}, based on a rearrangement of Eq 4 and incorporating the adsorption index:

$$x_s = 4\sqrt{\frac{kt_{eplf} / I_{ads}}{948\pi\phi\mu c_t}} \tag{14}$$

With the spacing thus determined, the well production forecast is computed for a single fracture to determine whether one fracture can produce sufficient revenue at least to pay for the fracture and horizontal segment it would require. If this test is passed, the number of fracture is increased until

- there are enough fractures to payout the well, or
- the number of fractures exceeds the input maximum number, or
- the well length exceeds the input maximum well length.

Figure 12 shows the input and output for the well design. Figure 13 shows the flow chart of the MTFW design strategy.

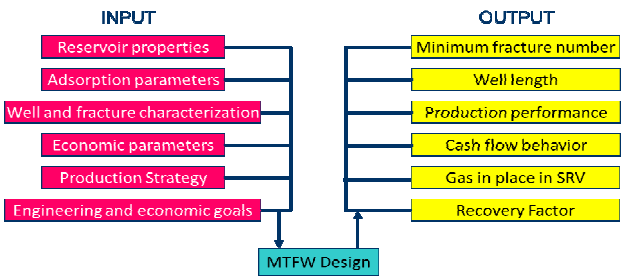

Figure 11. Input and Output of the MTFW design

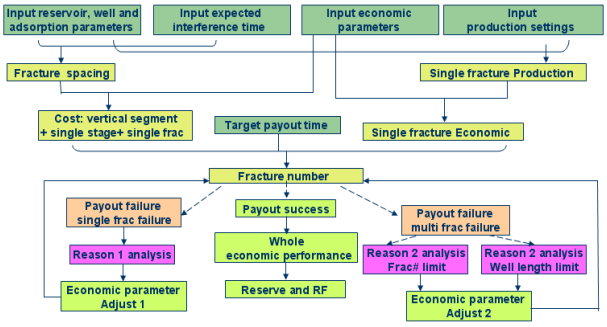

Figure 12. Flow Chart of MTFW Design

The fracture number calculation can fail to provide a result for the following reasons:

1. **Single Fracture Failure.** Production from each fracture must cover the cost of that fracture plus a portion of the cost to drill the vertical well segment. If the precondition $PV_{payout} > C_{ufrac} + x_s C_{uhw}$, which omits the vertical well cost altogether, cannot be satisfied for even one fracture, the more fractures are created, the greater will be the loss.
2. **Multiple Fracture Failure**.
   a. **Fracture number limit.** Theoretically, a minimum fracture number can be found to achieve the payout goal. However, there is a practical limit to the number of fractures. If the fracture number calculated exceeds the maximum fracture number allowed, an adjusted fracture cost or a horizontal drilling cost that could achieve the economic criteria can be computed.
   b. **Well length limit.** Again, a fracture number can be calculated. However, if the horizontal well length determined from the product of fracture spacing and number of fractures exceeds a maximum horizontal well length limit, as before an adjusted fracture cost or a horizontal drilling cost that could achieve the economic criteria can be computed.

After determining the fracture number, the geometry of the MTFW is determined. Multiplying the production rate for a single fracture by the fracture number provides the corresponding performances for the whole MTFW system. Moreover, the stimulated reservoir pore volume is determined from Eq 6 and gas in place within SRV, considering both free gas and adsorbed gas, can be calculated as:

$$GIP_{total} = GIP_{free} + GIP_{ads} = \frac{V_{SRV}\phi(1-S_w)}{B_{gi}} + V_{SRV}\rho_{rock}\frac{V_L p_i}{(p_L + p_i)} \tag{15}$$

The recovery factor is estimated using the cumulative production forecast computed down to an economic rate.

Well Design Examples

In this section we show 2 cases to illustrate the design process, one based on Haynesville Shale properties like those listed in Table 2, and the other based on New Albany Shale properties. Cases showing both successful and failed payout are shown. These designs assume $130/ft cost for drilling the vertical well segment and $220/ft for the horizontal segment. Also, the gas price is assumed to be $4/MSCF, 15% royalty and 5% discount rate.

Haynesville Shale Case

By entering the inter-fracture interference time determined from Eq. 6, we determined well designs for some of the cases shown in Figs. 7 and 11. Table 3 summarizes the design results.

Table 3: Haynesville Shale well designs

x_s	n_f	L_w	Payout time	C_{ufrac}	C_{total}	End time	Recovery
ft	1	ft	yr	$	$	yr	factor
207	11	2,277	6	100,000	2,770,879	32	97%
104	20	2,070	3	100,000	3,625,344	11	95%
52	40	2,070	3	12,000	2,105,345	3	60%

All of these designs target a 2000 ft horizontal well length. The above fracture spacing values are suitable for a longer well length: for example a 4000 ft well with twice as many fractures at the same cost per fracture would pay out in a similar time frame with double the rate and double the ultimate recovery.

This design sensitivity study shows that closer fracture or effective fracture spacing accelerates recovery. With 11 fractures spaced at about 200 ft, payout time is 6 years and after 32 years recovery efficiency is 97%, while with 20 effective fractures spaced at about 100 ft, the SRV is depleted to 95% recovery in only 11 years. For the 50 ft fracture spacing the fractures must cost considerably less, no more than $12,000 per fracture instead of the $100,000 per fracture assumed in the other two cases in the table. For this to be achievable, the 50 ft fracture density must be achieved as fracture complexity or by creating simultaneous multiple fractures in a single fracture stage. If an effective fracture spacing of 50 ft can be achieved at $12,000 per fracture, then the SRV would be depleted to only 60% recovery in 3 years. It would appear that increasing the design to 20 fractures makes sense, but the 40 effective fracture case appears to be neither economically feasible nor advisable from the recovery perspective.

The payout time for the 20 fracture well design makes it more attractive economically than the 10 fracture design. However, this design cannot be applied indiscriminately. To illustrate the importance of permeability, Fig. 13 compares the flow rate and cumulative production behavior for permeability values of 100, 10, and 1 nd. Clearly, if a template well design using 20 fractures is applied when the permeability is much lower than 100 nd, the well will not pay out until 30 years for the 10 nd permeability or until 300 years for 1 nd. This figure demonstrates the importance of determining permeability before executing the hydraulic fractures. A design for the 1 nd permeability indicates that a 4000 ft horizontal well with 41 1500 ft half-length fractures would pay out in 9 years if the fractures cost no more than $20,000 per fracture, but even after 100 years, the well will only have produced 42% of the gas in place. At 10 nd, a 3300 ft horizontal well with 32 1500 ft fractures would pay out in 4 years with fractures costing $100,000 per fracture and would produce 82% of the gas in the SRV after 30 years. The smaller permeability requires a larger SRV to be economic. If permeability is known before the fracture execution, perhaps the fractures can be designed accordingly.

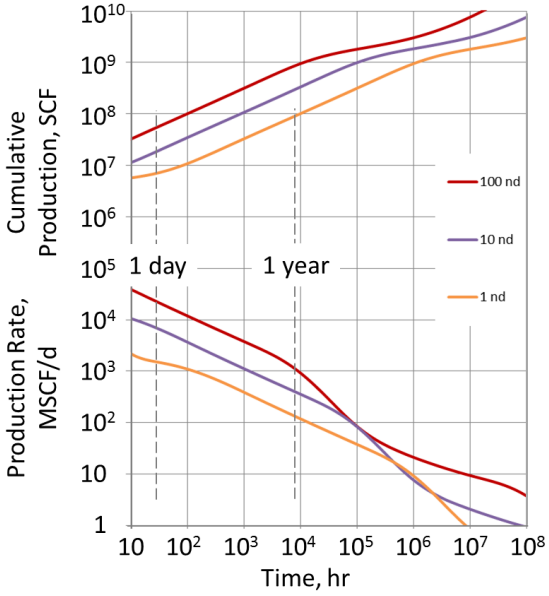

Figure 13: Rate decline and cumulative production for model inputs in Table 2, but with varying shale permeability.

New Albany Shale Case

The New Albany Shale reservoir is only 2380 ft deep and is underpressured at only 714 psi. Other well, reservoir, and economic parameters are shown in Table 4. Unlike the Haynesville Shale for which adsorption is believed to play little or no role, the adsorbed gas is essential to success in this play. Where the Haynesville proxy used for this paper has a pore volume of $5.53 \cdot 10^6$ ft^3 and 1.45 BSCF gas in place, the created SRV pore volume for this New Albany proxy has pore volume $4.30 \cdot 10^9$ ft^3 with 2.31 BSCF gas in place counting 1.40 BSCF adsorbed gas.

Assuming a 50 year inter-fracture interference time for 19 1200 ft half-length fractures in a 3100 ft horizontal well achieves payout in 12 years and recovers 53% of the gas in place, including adsorbed gas after 50 years on production. In this case 60% of the gas in place is originally in the adsorbed state.

Table 4. Parameters for MTFW Design in New Albany Shale

parameters	meaning	value	unit	parameters	meaning	value	unit
ϕ	reservoir porosity	0.06	fraction	C_{uwv}	unit length well cost (vertical segment)	200	$/ft
p_i	initial reservoir pressure	714	psia	C_{uwh}	unit length well cost (horizontal segment)	300	$/ft
h	pay zone thickness	56	ft	P_g	gas price (current)	5	$/Mscf
T	reservoir temperature	89	°F	$r_{royalty}$	payback ratio to royalty	25.00%	Percent
r_w	wellbore radius	4.5	inch	t_{payout}	expected payout time in years	300	Year
d	well depth	2380	ft	C_{ufrac}	unit fracture cost	200000	$
k	formation permeability	0.00018	md	r_{dis}	discount rate	5%	fraction
γ_g	gas specific gravity (air=1.0)	0.626	fraction	$Frac_{limit}$	fracture number limit	40	1
c_f	rock compressibility	3.0×10^{-6}	psi^{-1}	L_{limit}	horizontal well limit	10000	ft
p_L	Langmuir pressure	1044	psia	t_{eplf}	target fracture interference time in year	5	year
V_L	Langmuir Volume	125	scf/ton	x_f	single fracture half-length	1200	ft
ρ_{rock}	rock density	2.6	g/cc	p_{wf}	well bottom flow pressure	63	psia

Discussion

Instead of assuming a well drainage area and deciding how to drain it, the MTFW design method in this paper is providing a dynamic SRV determination method by calculating a minimum fracture number needed. This is not only because it is usually difficult to figure out a drainage area for a well in shale gas formation, but because the design is aimed to achieve the particular engineering (targeted interference time) and economic goal (targeted payout time). The reason to target the interference time is to ensure the well can recover a significant fraction of the gas in place in the SRV over its productive life.

In this design the shale formation permeability is important because it is directly used for the design of fracture spacing to meet the interference time goal and to forecast the production performance. However, the shale formation permeability is hard to determine because it is too low for laboratory measurement. Some operators are attempting to measure shale permeability from fracture calibration tests (Mohamed, *et al.* 2010).

Fracture half-length is another important information for this design strategy because it is directly related to the SRV. Accurate estimate for the achievable fracture half-length is challenging. Microseismic measurements that may give insight

into the real geometry of the created fractures in shale formations suggest they are complex. It is unknown whether microseismic indications of fracture extent are an indication of the productive fracture length.

The current efforts to place proppant in the fractures may be misplaced. It is imperative that operators evaluate the consistency between indications from microseismic measurements and from long term production behavior. The latter indicates clearly the extent of the SRV whenever pseudo pseudosteady state behavior is observed. For some wells this is in a matter of days or weeks. Once quantified from production data, the fracture half-length can be compared with microseismic indications. The timing of the start of pseudo pseudosteady state behavior enables estimation of permeability from production data. With this, it is possible to determine the effective number of fractures that have been created. In turn, it may be possible to evaluate the effective fracture widths. If the proppant volume is not consistent with this analysis, it begs the question whether the proppant is required, much as has been indicated previously for tight gas sand (Meyerhoffer and Meehan 1998).

Conclusions and Recommendations

Conclusions:

- Both free gas and adsorbed gas are present in shale gas reservoirs, and gas adsorption has varying impacts on the pressure investigation and production according to specific adsorption parameters and reservoir properties. We have quantified this effect with an adsorption index, for which we provided a correlation.
- MTFWs are widely applied in shale gas development, and the typical flow regimes during production (in order of appearance) include fracture storage, pseudolinear flow normal to transverse fracture, and pseudo pseudosteady state. Compound linear flow and infinite-acting or boundary flow according to particular outer boundary conditions have been shown for completeness, but typically an economic rate limit is reached before these flow regimes can be observed.
- During the pseudolinear flow, the product of total fracture half-length and square root of reservoir permeability is a constant. That means if either of them is known, the other one could be estimated. The pressure penetrates the formation at twice the rate of pressure penetration during radial or pseudoradial flow.
- The end of pseudolinear flow is dependent on the diffusivity coefficient. When this is observed in production data, the shale permeability can be estimated.
- The pseudo pseudosteady state trend defines the SRV pore volume. When ϕ and h are known, the fracture half-length can be determined from this flow regime trend. This trend, which others have called “transitional” is quite strategic for understanding the potential well recovery and recovery factor.
- We have presented an MTFW design strategy to meet specific engineering and economic criteria. Given an estimate for the shale permeability, the fracture spacing is determined from a designated time of interference between adjacent transverse fractures. The minimum number of fractures sufficient to pay out the well in a specified time is determined based on a simplified model for the production performance and the cost of each single fracture.
- Low production potential and high well cost can result in a failure of achieving the economic goal of payout in a targeted time. Reasons could be single fracture failure indicated when production from a single fracture cannot cover the horizontal drilling and fracturing cost for a single fracture stage, or multiple fracture failure when the number of fractures required to pay out the well within the specified time or the well length exceed designated values. The design strategy can provide insights on single facture costs or well costs that could make the process economically attractive for a specified natural gas price.
- Applying the design technique to the low pressure New Albany Shale showed that economics for this case are very marginal. Unless the costs of fractures and horizontal drilling are significantly decreased, it is difficult to achieve payout even after several years.
- Prospects for the Haynesville Shale are much better because high reservoir pressure provides much more gas in place within the SRV, resulting in production income that can easily cover the fracture and horizontal drilling cost for a 20-stage MTFW to achieve a 3-year payout goal if permeability is 100 nd. When permeability is as low as 1 nd, the economics are quite marginal and imply a much more aggressive well design.
- The importance of permeability to the well design cannot be overstated. Permeability variations in a given shale play imply a need to determine the local shale permeability and adjust the well design accordingly before drilling and fracturing execution.
- For the cases we have investigated, as long as the well is designed with fractures spaced sufficiently close to reach inter-fracture interference before the production rate declines below the economic limit rate, the well will recover at least 50% of the gas in place in the SRV. If inter-fracture interference does not occur, gas at the original reservoir pressure will be left behind.

Nomenclature

A_f	=	single fracture drainage area, ft^2
B	=	formation volume factor, res bbl/stb
B_g	=	gas formation volume factor, rcf/scf
B_{gi}	=	initial gas formation volume factor, rcf/scf
c_f	=	formation compressibility, psi^{-1}

c_t = total compressibility, psi^{-1}
C_{ads} = adsorption index correlation coefficient, cc/g
C_{ufrac} = unit fracture cost, $
C_{uhw} = unit horizontal well drilling cost, $/ft
C_{uvw} = unit vertical well drilling cost, $/ft
d = reservoir depth, ft
D_i = initial rate decline ratio, $year^{-1}$
$Frac_{limit}$ = fracture number limit
GIP_{ads} = adsorption gas in place, scf
GIP_{free} = free gas in place, scf
GIP_{total} = total gas in place, scf
h = payzone thickness, ft
h_{SRV} = thickness of stimulated reservoir volume, ft
I_{ads} = adsorption index
k = reservoir permeability, md
k_{ads} = slope coefficient of adsorption index correlation
L_w = horizontal well length, ft
L_{limit} = horizontal well length limit, ft
L_{SRV} = length of stimulated reservoir volume, ft
m_{lf} = slope of straight line for linear flow on the coordinate of Δp versus $t^{1/2}$, $psi/hour^{1/2}$
$m(p)$ = real gas pseudo pressure, psi^2/cp
$MTFW$ = multiple transverse fracture horizontal well
n_f = fracture number
P_g = current natural gas price, $/Mscf
p_i = initial reservoir pressure, psia
p_L = Langmuir pressure, psia
p_{wf} = well bottomhole pressure, psia
PDD = pressure drawdown
PV = present value
q_g = gas production rate, Mscf/d
q_{gt} = total gas production rate by all the transverse fractures, Mscf/d,
Q_a = annual gas cumulative production, scf
r_{dis} = discount rate, percentage
$r_{royalty}$ = royalty ratio, percentage
r_w = wellbore radius, inch
SRV = stimulated reservoir volume
S_w = water saturation, fraction
t = time, year or hour
t_{eplf} = end of pseudolinear flow, year
t_{payout} = payout time, year
T = reservoir temperature, ºF
V_p = pore volume, scf/ton
V_L = Langmuir Volume, scf/ton
V_{sr} = stimulated reservoir volume, ft^3
V_{SRV} = volume of stimulated reservoir volume, ft^3
w_{SRV} = width of stimulated reservoir volume, ft
x_f = transverse fracture half-length, ft
x_{ft} = total fracture half-length, ft
x_i = pressure investigation distance, ft
x_s = fracture spacing, ft

Greek variables

ϕ = porosity, fraction
μ = viscosity, cp
μ_g = gas viscosity, cp
γ_g = specific gas gravity, fraction
ρ_{ads} = adsorption density, g/cc
ρ_{rock} = rock density, g/cc
σ = adsorption index correlation coefficient

Subscripts

a	=	annual
ads	=	adsorption
dis	=	discount
f	=	fracture or formation
L	=	Langmuir
eplf	=	end of pseudolinear flow
p	=	pore
payout	=	payout time
SRV	=	stimulated reservoir volume
royalty	=	royalty
t	=	total
u	=	unit
w	=	well

Acknowledgements

We would like to thank Miss. C. Angelica in Gas Technology Institute (GTI) and Mr. R. Hamilton in NGAS for providing guidance in the New Albany Shale study. We would also like to thank Shell Oil Company for sharing production data from the Haynesville Shale. We also express our appreciation to Kappa Engineering for the technical support during the research and for use of the Ecrin software. Moreover, we would like to thank Dr. B. Wattenbarger of Texas A&M University for his help.

References

Al-Kobaisi, M., Ozkan, E., Kasogi, H., and Ramirez, B. 2006. Pressure-Transient Analysis of Horizontal Wells with Transverse, Finite-conductivity Fractures. Paper PETSOC 2006-126 presented at the Petroleum Society's 7th Canadian International Petroleum Conference (57th Annual Technical Meeting), Calgary, Alberta, Canada, 13-15 June.

Arthur, J.D., Bohm, B., and Layne, M. 2008. Hydraulic Fracturing Considerations for Natural Gas Wells of the Marcellus Shale. Paper presented at the Ground Water Protection Council 2008 Annual Forum, Cincinnati, Ohio, 21-24 September.

Cipolla, C.L., Lolon, E.P., Erdle, J.C., and Rubin. B. 2009. Reservoir Modeling in Shale-Gas Reservoirs. Paper SPE 125530 presented at the 2009 SPE Eastern Regional Meeting, Charleston, West Virginia, 23-25 September.

Clarkson, C.R., Jordan, C.L., Ilk, D., and Blasingame, T.A. 2009. Production Data Analysis of Fractured and Horizontal CMB Wells. Paper SPE 125929 presented at the 2009 SPE Eastern Regional Meeting, Charleston, West Virginia, 23-25 September.

Economides, M. J., Hill, A. D. and Ehlig-Economides, C. E.: *Petroleum Production System*, Prentice Hall PTR, Upper Saddle River, New Jersey, 1993.

Ehlig-Economides, C.A. 1992. Computation of Test Area of Investigation in Nonradial Geometries. Paper SPE 25020 presented at the European Petroleum Conference, Cannes, France, 16-18 November.

Freeman, C.M., Moridis, G., Ilk, D., and Blasingame, T.A. 2009. A Numerical Study of Performance for Tight Gas and Shale Gas Reservoir Systems. Paper SPE 124961 presented at the 2009 SPE Annual Technical Conference and Exhibition, New Orleans, Louisiana, 4-7 October.

Kuuskraa, V.A., Sedwick, K., and Yost II, A.B. 1985. Technically Recoverable Devonian Shale Gas in Ohio, West Virginia and Kentucky. Paper SPE 14503 presented at the SPE 1985 Eastern Regional Meeting, Morgantown, West Virginia, 6-8 November.

Lane, H.S., Watson, A.T., and Lancaster, D.E. 1989. Identifying and Estimating Desorption from Devonian Shale Gas Production Data. Paper SPE 19794 presented at the 64th Annual Technical Conference and Exhibition of the Society of Petroleum Engineers, San Antonio, TX, 8-11 October.

Lee, J., Rollins, J. B., and Spivey, J. P. 2003. *Pressure Transient Testing*. Textbook Series, SPE , Richardson, Texas 9: 119.

Mayerhofer, M.J., and Meehan, N.D.: "Waterfracs – Results from 50 Cotton Valley Wells," Paper SPE 49104 presented at the 1998 SPE Annual Technical Conference and Exhibition held in New Orleans, Louisiana, 27-30 September 1998.

Mayerhofer, M. J., Lolon, E.P., Warpinski, N. R., Cipolla, C.L., and Walser. D. 2008. What is Stimulated Reservoir Volume

(SRV)? Paper SPE 119890 presented at the 2008 SPE Shale Gas Production Conference, Fort Worth, TX, 16-18 November.

Mohamed, I.M., Nasralla, R.A., Sayed, M.A., Marongiu-Porcu, M., and Ehlig-Economides C.A.: "Evaluation of After-Closure Analysis Techniques for Tight and Shale Gas Formations," paper SPE 140136 to be presented at the SPE Hydraulic Fracturing Technology Conference and Exhibition held in The Woodlands, Texas, USA, 24–26 January 2011.

Pope, C. D., Palisch, T. T., Lolon, E. P., Dzubin. B. A., and Chapman, M. A. 2010 Improving Stimulation Effectiveness-Field Results in the Haynesville Shale. Paper SPE 134165 presented at the 2010 Annual Technique and Exhibition, Florence, Italy, 12-22 September.

Schepers, K.C., Gonzalez, R.J., Koperna, G.J., and Oudinot. A.Y. 2009. Reservoir Modeling in Support of Shale Gas Exploration. Paper SPE 123057 presented at the 2009 SPE Latin American and Caribbean Petroleum Engineering Conference, Cartagena, Colombia, 31 May- 3 June.

Wei, Y., and Economides, M.J. 2005. Transverse Hydraulic Fractures from a Horizontal Well. Paper SPE 94671 presented at the 2005 SPE Annual Technical Conference and Exhibition, Dallas, Texas, 9-12 October.

Zuber, M.D., Williamson. J.R., Hill. D.G., Sawyer, W.K., and Frantz. J.H. 2002. A Comprehensive Reservoir Evaluation of a Shale Reservoir-The New Albany Shale. Paper SPE 77469 presented at the 2002 SPE Annual Technical Conference and Exhibition, San Antonio, Texas, 29 September-2 October.